Table S1. List of experiments in which each tissue sample was used and observed GAS growth on the relevant tissue sample

Sample [A]	Figure	GAS multiplication observed by live imaging	GAS multiplication observed in static conditions	GAS multiplication observed in supernatant
S#16	Fig. 1A, Fig. 1H, Fig. 2A-C, Fig. S2, Fig. S3C	YES	YES	nt[C]
S#20	Fig. 1B Fig. S3B	na[B]	na	nt
S#1	Fig.S2A	na	na	nt
S#9	Fig. 1C-D, Fig. 1G-J, Fig. 2B-D, Fig. 4B-C, Fig. S2, Fig. S4, Table S3-6, Supp video 1	YES	YES	YES
S#10	Fig. 1D, Fig. 1H-J, Fig. 4B-C, Fig. S4, Table S3-6	YES	na	YES
S#7	Fig. 1H-J, Fig. 3C, Fig. 4B-C, Fig. S4, Table S3-6	YES	na	NO
S#17	Fig. 1H, Fig. 3D, Fig. 3G	YES	na	nt
S#8	Fig. 1I-J, Fig. 2B-C, Fig. 4B-C, Fig. S2, Fig. S4, Table S3-6	na	YES	NO
S#5	Fig. 1D, Fig.2E, Fig. 3E, Fig. S3B	YES	na	nt
S#18	Fig. 1D-F, Supp video 2	YES	na	nt
S#19	Fig. 1D, Fig. 3A, Supp video 3	YES	na	nt
S#2	Fig. 1I, Fig. 2B, Fig. 3B, Fig. 4A, Fig. S2, Table S2	na	YES	YES
S#3	Fig. 1I, Fig. 4A, Table S2	na	na	YES
S#4	Fig. 1I, Fig. 4A, Table S2	na	na	YES
S#6	Fig. 1I, Fig. 4A, Table S2	na	na	NO
S#12	Fig. 3G	na	na	nt
S#13	Fig. 3E	na	na	nt
S#14	Fig. 3E	na	na	nt
S#15	Fig. 3G, Fig. S2	na	YES	nt
S#21	Fig. 3G	na	na	nt

[A] Samples with different numbers are from different subjects. The numbering does not correspond to the order in which subjects were included in the study.

[B] NA, not applicable. The sample had either not been analyzed by live imaging or not been observed at two time points.

[C] NT, not tested

Table S2. Comparison of the overexpression of genes involved in the immune response

	GAS		GBS	
	mRNA Fold-change	***p-value***	**mRNA Fold-change**	***p-value***
IL6	3.44	0.2443517	20.08	0.0000001
IL1B	**6.06**	**0.0101306**	**7.79**	**0.0000004**
TNF	**40.37**	**0.0106377**	**32.25**	**0.0000016**
CXCL2	**29.34**	**0.0005470**	**10.46**	**0.0000044**
CCL20	**12.77**	**0.0005246**	**33.91**	**0.0000144**
CXCL8	1.90	0.0911197	4.80	0.0000319
IL1RN	0.94	0.9482826	3.96	0.0000747
CCL4	**111.43**	**0.0032225**	**12.69**	**0.0000815**
IL1A	1.83	0.4538192	6.85	0.0001290
NFKB1	1.11	0.6764782	2.25	0.0001450
ICAM1	2.08	0.4791674	5.01	0.0001730
NFKBIA	2.75	0.0500612	5.51	0.0001780
CXCL3	**28.34**	**0.0000184**	**9.92**	**0.0001850**
TLR2	1.26	0.7816158	4.52	0.0002380
TLR6	1.15	0.7529346	0.43	0.0017900
CCL13	0.76	0.7698270	0.47	0.0018400
NLRP3	2.36	0.0521823	4.39	0.0022200
CCR7	2.62	0.1155378	3.36	0.0064500
CCR1	2.00	0.0623347	0.36	0.0065000
CCL3	**14.52**	**0.0009604**	**4.88**	**0.0072300**
CD80	1.61	0.5656690	3.08	0.0081700
CD14	0.53	0.5807491	0.64	0.0084000
IFNA2	0.84	0.8758766	0.71	0.0125000
CCL2	2.58	0.2099790	2.38	0.0137000
CCL8	1.71	0.5478146	3.10	0.0146000
IL10RA	0.56	0.2238125	1.55	0.0186000
CXCL1	**14.52**	**0.0007640**	**3.20**	**0.0200000**
TICAM1	0.87	0.7283693	1.69	0.0226000
IL23A	**9.47**	**0.0229023**	**13.52**	**0.0229000**
CXCL5	1.48	0.5061415	2.98	0.0233000
IL37	0.64	0.1534900	0.68	0.0356000
CD40LG	2.38	0.3139426	0.74	0.0411000
IL18	1.19	0.7368512	2.15	0.0510000
LTA	0.35	0.2617627	1.42	0.0511000
TLR8	0.94	0.9689146	1.72	0.0609000
CXCR2	0.51	0.3713690	0.54	0.0629000
NOD1	0.78	0.5487833	0.60	0.0639000
CXCR3	1.58	0.4743766	0.77	0.0803000
IL9R	0.23	0.1263553	1.27	0.0815000
IRAK1	0.69	0.3244791	0.74	0.0861000
TLR4	1.40	0.4818540	0.63	0.0879000
TBX21	1.09	0.9344079	0.75	0.0966000
RAG1	0.74	0.5642718	0.80	0.1000000
CSF2	1.18	0.8418437	1.33	0.1030000
IFNGR1	0.74	0.3574953	1.25	0.1120000
STAT3	1.21	0.4820490	1.27	0.1330000
CXCL10	3.57	0.4609962	5.21	0.1360000
TLR1	0.93	0.9379901	0.70	0.1380000
CASP1	0.76	0.7458079	1.42	0.1440000
CD86	0.94	0.9553241	0.64	0.1730000
IL10	**4.73**	**0.0490744**	**1.43**	**0.2190000**

The mean value of the fold change is that calculated from the data shown Figure 4A for GAS (n=4) published in Park et al (1) for GBS (n=4). In green and bold the genes significantly upregulated after infection with GAS and GBS compared to non-infected samples; in orange the genes significantly only upregulated after infection with GBS. In red and bold, the gene only upregulated after GAS infection. Hits were classified in the decreasing order of *p-value* for GBS, until no gene was significantly differentially regulated for GAS and GBS.

Table S3. Concentration of inflammatory molecules in the supernatants at 4 h

	CT	WT	ΔSLO	ΔSpeB
TNF	**1.9** (0.25-2.9 ±0.6)	**130** (31-287 ±60.8)	**23** (3.7-70 ±15.8)	**58** (6.9-161 ±35)
CCL3	**11** (3.9-16 ±2.9)	**186** (40-481 ±102)	**31** (8-92 ±20)	**82** (18-250 ±56)
CXCL2	**323** (81-444 ±84)	**544** (158-1091 ±222)	**167** (42-441 ±92)	**340** (132-629 ±104)
CCL20	**13** (2-21 ±4)	**9.6** (2.2-23 ±4.6)	**3.5** (1.6-7.1 ±1.3)	**8.2** (5.1-11 ±1.2)
IL-1β	**3.7** (2.8-4.9 ±0.44)	**11** (5.2-25 ±4.5)	**9.7** (2.6-18 ±3.3)	**18** (5.7-39 ±7.4)
IL-6	**267** (60-417 ±75)	**346** (46-778 ±159)	**106** (21-145 ±29)	**279** (107-393 ±68)

Concentration in pg/mL. Results are expressed as: Mean (minimum-maximum ± standard error). 4 samples.

Table S4. Concentration of inflammatory molecules in the supernatants at 8 h

	CT	WT	ΔSLO	ΔSpeB
TNF	**1.5** (0.1-2.8±0.6)	**401** (17-1090 ±246)	**320** (83-622 ±118)	**938** (152-1798 ±372)
CCL3	**12** (5.4-19 ±2.8)	**616** (18-1908 ±437)	**503** (73-761 ±158)	**1202** (279-2192 ±391)
CXCL2	**576** (291-1077 ±172)	**932** (153-2311 ±482)	**1115** (487-2115 ±351)	**3078** (410-7190 ±1453)
CCL20	**24** (5-55 ±11)	**33** (1.6-85 ±18)	**33** (3.1-79 ±17)	**147** (13-429 ±98)
IL-1β	**3.9** (1.6-6.9 ±1.2)	**43** (19-69 ±10)	**49** (15-97 ±18)	**75** (27-154 ±29)
IL-6	**602** (448-904 ±102)	**951** (222-2203 ±432)	**1202** (495-2127 ±401)	**2274** (359-4283 ±853)

Concentration in pg/mL. Results are expressed as: Mean (minimum-maximum ± standard error). 4 samples.

Table S5. Concentration of antimicrobial peptides in the supernatants at 4 h

	CT	WT	ΔSLO	ΔSpeB
hBD1	**2212** (313-3369 ± 661)	**2807** (379-6579 ± 1324)	**934** (69-1378 ± 305)	**2923** (1045-3848 ± 636)
hBD2	**4599** (2376-6405 ± 885)	**5356** (1862-8029 ± 1423)	**6288** (1862-11719 ± 2049)	**963** (301-1773 ± 304)
LL37	**1.1** (0.36-2.1 ± 0.51)	**1.3** (0.61-2.2 ± 0.38)	**1.2** (0.31-2.7 ± 0.54)	**2.2** (0.71-5 ± 0.97)

Concentration in pg/mL. Results are expressed as: Mean (minimum-maximum ± standard error). 4 samples

Table S6. Concentration of antimicrobial peptides in the supernatants at 8 h

	CT	WT	ΔSLO	ΔSpeB
hBD1	**4365** (2888-5561 ± 552)	**5072** (1677-7020 ± 1169)	**11102** (6402-12948 ± 1571)	**8998** (5193-13317 ± 2207)
hBD2	**15146** (7426-29730 ± 5162)	**39634** (9835-89457 ± 39634)	**13077** (3527-32273 ± 13077)	**25009** (7706-52619 ± 10216
LL37	**1.6** (0.56-3.2 ± 0.62)	**1.8** (0.26-4.3 ± 0.89)	**1.7** (0.49-3.2 ± 0.68)	**2.3** (0.91-3.2 ± 0.49)

Concentration in pg/mL. Results are expressed as: Mean (minimum-maximum ± standard error). 4 samples

Table S7. Strains and plasmids used in this study

Strains or plasmid	Relevant properties	Source or reference
Streptococcus pyogenes		
M28PF1	Wild-type representative *emm28* clinical isolate	(2)
ΔSpeB	M28PF1 deleted from nt 72 to nt 1155 of the *speB* gene coding for SpeB	This study
ΔSLO	M28PF1 deleted from nt 76 to nt 1690 of the *slo* gene coding for SLO	This study
BTSLO	Back-to-the-wild-type, the reverting strain of the ΔSLO construction	This study
M28PF1-GFP	M28PF1 with the integrated pG1-lacA-PTetO-gfp	This study
ΔSpeB-GFP	ΔSpeB with the integrated pG1-lacA-PTetO-gfp	This study
Plasmids		
pG+host5	Erm; ColE1 replicon, thermosensitive derivative of pGK12; MCS pBluescript	(3)
pATΩgfp	pAT28 derivative containing the *gfp* gene	(4)
pTCV_TetO	Plasmid containing the tetO tetR Pxyl promoter, inducible with anhydrotetracycline	(5)
pG1-Perm-gfp	pG+host5 containing the *gfp* gene from pATΩgfp	This study
pG1-lacA-Perm-gfp	pG1-Perm-gfp with the lacA intergenic region to allow stable integration in GAS genome	This study
pG1-lacA-PTetO-gfp	pG1-lacA-Perm-gfp with the Erm promoter replaced by the tetO tetR Pxyl promoter of pTCV_TetO. Can be integrated in GAS genome for anhydrotetracycline inducible *gfp* expression	This study

Table S8. Primers used in this study for cloning and checking cloning

Primer Name	Sequence*	Orientation, Localization / gene start codon
F_tetO	GTGGAATTGTGAGCGGATAAC	NA
R_tetO	**GGTACC**TTTTCACTCGTTAAAAAGTTTTGAGAATATTTTATATTTTTGTTCATGTAATCACTCCTTCTTAATCTGTTAACGCTACGATCTAGCT	NA
F_lacA	ACATGATTACGAATTTCAACGACTTCGTATTTACCTT	Reverse, 92 nt
R_lacA	ACACTCTTAAGAATTCGCGGTCATATCTGAGATGTT	Direct, 551 nt
R_extlacA	CCACCATGGGTCCTGATA	Direct, 609 nt
RP48	AGCGGATAACAATTTCACACAGGA	NA
SLO-F1	GACTCTAGA**GGATCC**GGTGCCAAAGGGTTTAGAA	Direct, 492 nt
SLO-R1	CTCAGGGGGATAAGAGCTGCCGTTAGTAG	Reverse 75 nt
SLO-F2	TCTTATCCCCTGAGCCCATATGGTTCGAT	Direct, 1690 nt
SLO-R2	CATGATTAC**GAATTC**GGGACAGTTGGGGTCAAATC	Reverse 2179 nt
SpeB-F1	GACTCTAGA**GGATCC**GAGCATCTACTAGCCACAATA	Direct, 531 nt
SpeB-R1	GGGTTAGCAAGAACAAATCC	Reverse, 71 nt
SpeB-F2	TGTTCTTGCTAACCCTTCAACGGTTACCAAAGTGC	Direct, 1155 nt
SpeB-R2	CATGATTAC**GAATTC**ATTAGTAGGCGTTGATGACC	Reverse, 1676 nt

* restriction enzyme sites are highlighted in bold and sequences used for the In-fusion© cloning are shown in red.

References of supplementary tables:

1. Park H-R et al. Group B *Streptococcus* activates transcriptomic pathways related to premature birth in human extraplacental membranes *in vitro*. *Biol Reprod*. 2018;98(3):396–407
2. Longo M et al. Complete Genome Sequence of *Streptococcus pyogenes emm28* strain M28PF1, responsible of a puerperal fever. *Genome Announc*. 2015;3(4):e00750-15.
3. Biswas I, Gruss A, Ehrlich SD, Maguin E. High-efficiency gene inactivation and replacement system for gram-positive bacteria. *J Bacteriol*. 1993;175(11):3628–3635.
4. Clarebout G, Leclercq R. Fluorescence assay for studying the ability of macrolides to induce production of ribosomal methylase. *Antimicrob Agents Chemother*. 2002;46(7):2269–2272.
5. Buscetta M et al. FbsC, a novel fibrinogen-binding protein, promotes *Streptococcus agalactiae*-host cell interactions. *J Biol Chem*. 2014;289(30):21003–21015.

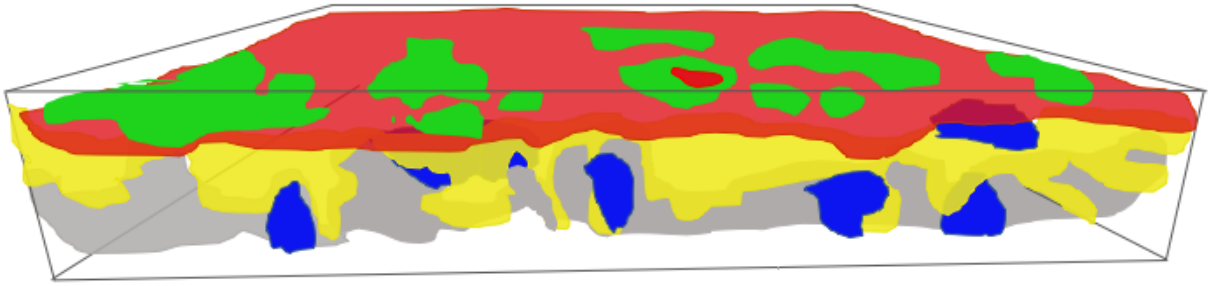

Figure S1. Schematic reproduction of the Imaris 3D representation in Figure 1A. The border of the cells could not be precisely delineated by this approach that did not label their surface. The volume they occupy is grossly indicated. Green, GAS; red, fibronectin, yellow, collagen; blue, nuclei; grey, cellular layer.

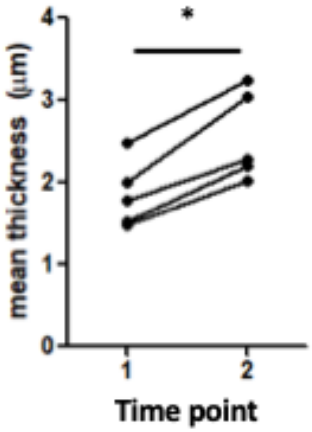

Figure S2. GAS grows *ex vivo* on decidual tissues in static conditions. Decidual tissues were infected and images taken at 2 time points. Mean thickness was evaluated as in figure 1H; mean values of 5 to 7 fields for each time point. Statistical analysis: Mann-Whitney U test, one-way; *, $p<0.05$.

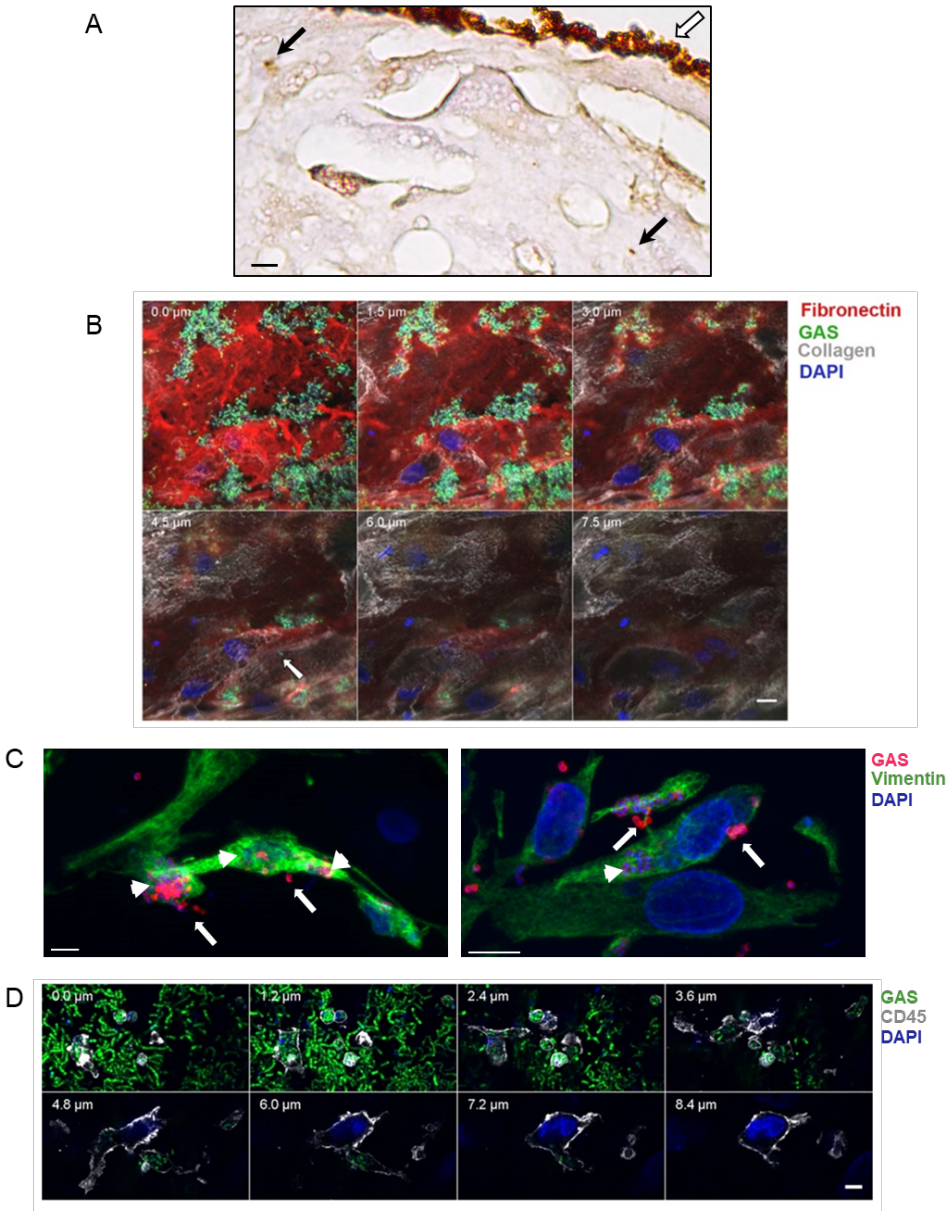

Figure S3. GAS invades the tissue and is found as extra- or intracellular bacteria, in stromal and immune cells. **A**, Immunohistochemical staining of GAS on the decidua 4h pi static conditions. White arrow, colonies at the surface of the tissue; black arrows tissue invading bacteria. Anti-GAS antibodies were used and secondary antibodies were detected with DAB as a chromogen (brown deposits correspond to signal) Scale: 10 µm. Magnification: 100 X. **B**, ImageJ montage of an infected tissue at 16 h pi static conditions. Anti-fibronectin, red; anti-type IV collagen, grey; GFP-WT, green; DAPI, blue; white arrow, a GFP-WT coccus, the 4.5 is the same slice as that shown Figure 2A. Scale bar: 10 µm. Magnification: 40 X. **C**, Immunofluorescence of the decidua 16 h pi static conditions. Stromal cells are vimentin +; vimentin, green; GAS, detected by anti-GAS antibodies, magenta; DAPI, blue; white arrows, bacteria in direct contact with stromal cells; arrowheads bacteria inside stromal cells. Scale bar 10 µm. Magnification: 100 X., **D**, ImageJ montage of an infected tissue 3 h pi flow conditions. The 4.8 m is the same slice as that shown Figure 2E. Anti-CD45, grey; GFP-WT, green; DAPI, blue. Scale bar: 5 µm. Magnification: 100 X. **B & D,** each corresponds to a single field at multiple depths. The depths are indicated at the top left of each panel. 0 corresponds to the first appearance of the GAS layer and is the first slice shown. All images are single slices acquired with a z-step of 0.3 µm.

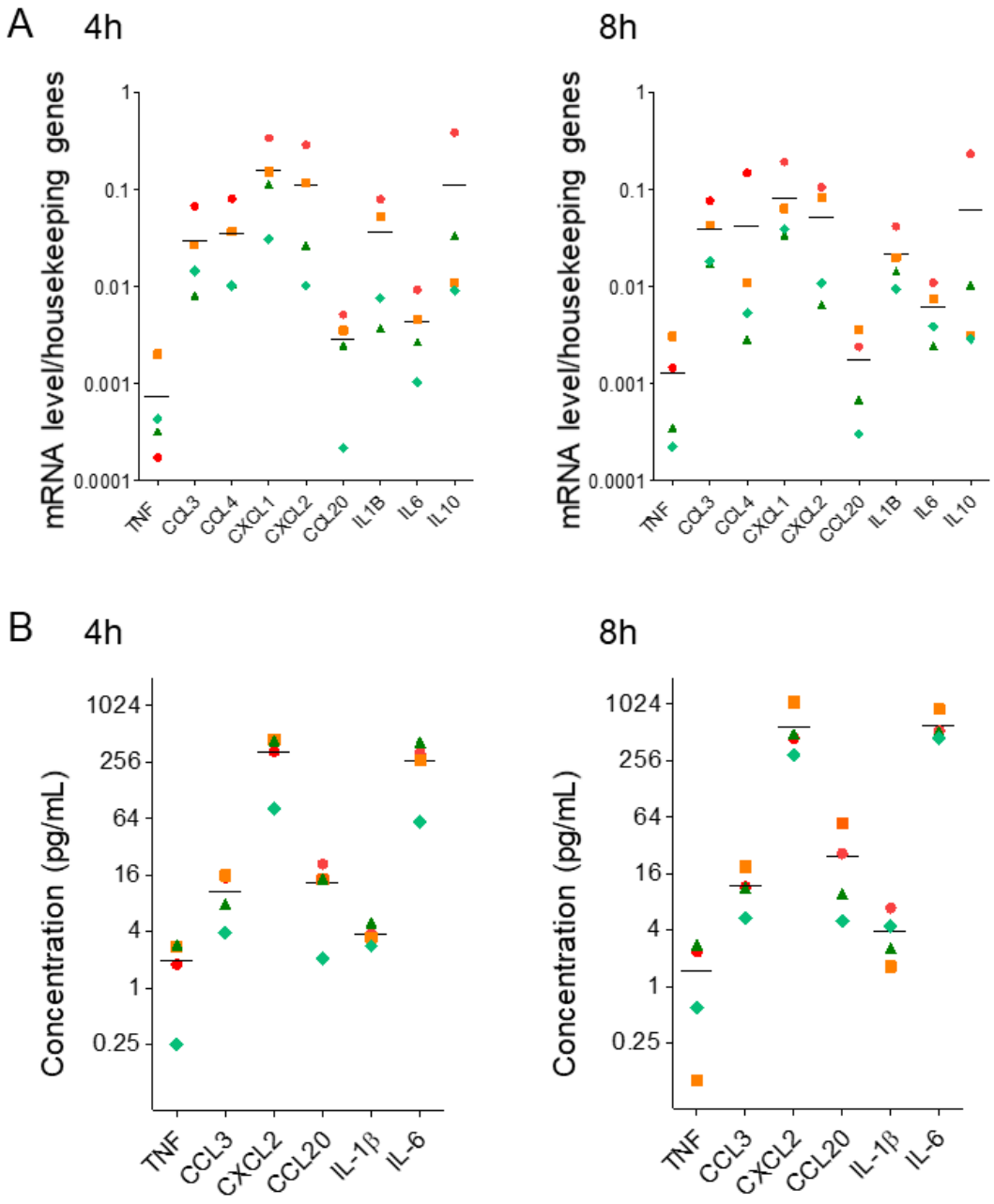

Figure S4. Basal levels expression of cytokine genes (A) and accumulation of the cytokines in non-infected tissues (B). A, Basal level of expression of the indicated immune-related genes in the non-infected conditions, at 4 (left panel) and 8 h (right panel) post-experiment starting point, compared to the housekeeping genes. B. Basal levels of accumulation of the indicated cytokine peptide 4 h (left panels) and 8 h (right panels) in the supernatant of non-infected decidual tissues. Symbols as in Figure 5B.

Supplementary video:

Supp video 1. GAS multiplication at the tissue surface
Live confocal microscopy of the human decidua infected by GAS under flow conditions, acquired *en face*. GAS is in green. Magnification: 25 X. Scale bar: 20 µm. Time step = 30 minutes. The images are the same as in Figure 1C and are a z-max intensity projection.

Supp video 2. Isolated GAS multiplication at the tissue surface
Live confocal microscopy GAS is in green of the human decidua infected by GAS under flow conditions, acquired *en face*. Magnification: 25 X. Scale bar: 5 µm. Time step = 30 minutes. The images are the same as in Figure 1E and are a z-max intensity projection..

Supp video 3. Immune cell blebbing and death after infection
Live confocal microscopy of tissue infected under flow conditions. Intact nucleus, red (Draq5); permeabilized nucleus (dead cell), blue; CD45 (immune cells), yellow. Magnification: 25 X. Scale bar: 10 µm. Time step = 30 minutes. The images are a z-max intensity projection.